INTERNATIONAL JOURNAL OF AUTOMOTIVE AND MECHANICAL ENGINEERING
ISSN: 2229-8649 e-ISSN: 2180-1606
VOLUME 22, ISSUE 2, 2025, 12359 - 12372
DOI: https://doi.org/10.15282/ijame.22.2.2025.9.0946

RESEARCH ARTICLE

Vibrational Energy Harvesting from Functionally Graded Nonprismatic Beams

Alok Ranjan Biswal, Deepak Ranjan Biswal*

Faculty of Mechanical Engineering, DRIEMS University, Cuttack, Odisha,754022, India

ABSTRACT – This study investigates the vibrational energy harvesting capabilities of axially functionally graded nonprismatic piezolaminated beams under combined thermal-mechanical loading conditions for automotive applications. A coupled multi-physics finite element model was developed to analyze the electromechanical response of tapered cantilever beams with varying width (c_b) and height (c_h) taper coefficients while maintaining a material gradient index (k=1) and power law exponent (np=4). Four geometric configurations with taper coefficients of 0.3 and 0.7 were subjected to both isolated mechanical impulses loading and combined thermal-mechanical loading with a 50°C temperature gradient. Results demonstrate that taper parameters significantly influence performance, with height tapering showing greater impact on displacement response than width tapering. Thermal loading increased displacement by 16.7-66.7% across configurations, highlighting complex thermal-mechanical coupling effects. Voltage generation was enhanced with increasing taper coefficients, reaching 340 V/mm in the optimized configuration (c_b =0.7, c_h =0.7) compared to 140 V/mm in the baseline configuration (c_b=0.3, c_h=0.3). Most notably, output power exhibited dramatic enhancement under combined loading conditions, with the optimized configuration achieving 0.15 W/mm², representing a 650% increase over mechanical loading alone. The findings suggest that axially functionally graded nonprismatic piezolaminated beams offer promising solutions for harvesting waste vibrational and thermal energy in automotive environments, with the potential to power various low-energy automotive sensors and monitoring systems.

ARTICLE HISTORY

Received : 13th June 2024
Revised : 14th Apr. 2025
Accepted : 08th May 2025
Published : 12th June 2025

KEYWORDS

Energy harvesting
Finite element analysis
Genetic algorithm
Nonprismatic beam
Piezoelectric

1. INTRODUCTION

Energy harvesting has been extensively used for the last few decades to provide an alternative energy source for microelectro-mechanical systems (MEMS). Energy harvesting in automotive applications enhances vehicle efficiency by converting vibrational energy from road conditions and engine operations into usable electrical power. This energy can power sensors, reduce battery load, and improve overall vehicle performance, contributing to more sustainable and efficient automotive technologies. MEMS in battery-operated automobiles enhance performance by enabling precise sensing and control. They optimize battery management, monitor vehicle dynamics, and improve safety systems, contributing to efficient energy use and extended battery life, thus supporting the development of advanced, reliable electric vehicles. For this purpose, piezoelectric materials show a crucial role due to its significant behavior. The progress in the piezoelectric-based energy harvesting field has been thoroughly reviewed and discussed. Ali et al. [1] recently proposed developments in piezoelectric wearable energy harvesting from human motion. While this review highlights significant progress in piezoelectric wearable energy harvesting technology, it also identifies areas ripe for further development. Optimizing energy conversion efficiency, enhancing material durability, and integrating seamlessly with various wearable devices are exciting opportunities for future research. Additionally, overcoming miniaturization challenges and improving user comfort will drive the next wave of innovation in this field. Aabid et al. [2] proposed a detailed study of piezoelectric energy harvesters (PEHs). The article systematically explains the fundamental concepts and modeling of piezoelectric materials, summarizes previous studies and applications of PEHs, and critically discusses current challenges in the field. While the article focuses primarily on PEHs, it may potentially overlook other smart materials.

Additionally, the review may not cover the latest advancements due to the rapid developments in the field. However, their review demonstrates notable limitations in scope by prioritizing piezoelectric materials while inadequately addressing alternative smart materials with comparable potential. Furthermore, the rapid pace of technological development in this domain likely renders portions of their analysis outdated. Covaci et al. [3] reviewed the current energy harvesting methods, focusing on piezoelectric energy harvesting. It examines the direct piezoelectric effect, explores various piezoelectric transducers, and discusses modeling their behavior in time and frequency domains. Additionally, it presents circuits designed to maximize harvested energy. While their examination of the direct piezoelectric effect and various transducer configurations provides valuable insights, their analysis of circuit optimization techniques lacks rigorous quantitative comparisons between different approaches. Askari et al. [4] presented a study on vibration energy harvesting using piezoelectric bimorph plates, proposing a comprehensive two-dimensional model. This model, incorporating various material properties, configurations, and structural damping, provides analytical expressions for

***CORRESPONDING AUTHOR | D.R.Biswal |** ✉ deepakrbiswal@gmail.com

voltage output and vibration response under harmonic input. It aims to validate the model and explore power generation performance, though potential limitations and challenges are not discussed. Though mathematically comprehensive in incorporating material properties and structural damping, their model insufficiently addresses non-linear behaviors under real-world conditions

Iqbal et al., in 2021, reviewed and analyzed recent developments in vibration-based energy harvesting (VEH), focusing on piezoelectric, electromagnetic, and hybrid piezoelectric-electromagnetic harvesters. It evaluated various prototypes based on device architecture, conversion mechanisms, performance parameters, and implementation. This research provides insights into optimizing VEH systems for the sustainable operation of wireless sensor nodes (WSNs), highlighting their potential to replace batteries and reduce environmental impact by harnessing ambient vibration energy. Although the work provides a useful foundation for understanding diverse harvesting mechanisms, it presents a limited critical discussion of scaling limitations that hinder widespread commercial adoption [5]. In their study, V. N. Burlayenko and colleagues [6] utilized ABAQUS to compare the simulation of free vibrations in axially functionally graded material (AFGM) beams with nonuniform cross-sections, examining both one-dimensional (1D) and three-dimensional (3D) models. By solving the eigenvalue problem, they determined natural frequencies and mode shapes. UMAT subroutines implemented material gradients, revealing that model distinctions grow with geometric complexity and material inhomogeneity, especially for high-frequency modes. The eigenvalue problem solution provides natural frequencies and mode shapes but fails to adequately validate computational results against experimental data, raising questions about real-world applicability. Wu et al. [7] explored high-power output potential from piezoelectric mechanisms in engineering structures, reviewing techniques to enhance energy harvesting.

Focusing on structural design, the study examined methods to increase power generation by enhancing operation frequency and strain levels on piezoelectric materials. Findings suggest that advanced designs and additive manufacturing can significantly improve efficiency, achieving higher power outputs in engineering applications. A review of key parameters influencing piezoelectric energy harvesting performance and the provision of guidelines for future development is proposed by T. Li and PS Lee [8]. A universal theoretical model is developed to categorize parameters into six groups, including material properties, structural designs, excitation sources, frequency and speed effects, electrical load effects, and energy accumulation methods in the proposed research. Each group is analyzed and discussed. The study provides insights and practical guidelines to enhance piezoelectric energy harvesting technology, highlighting potential applications and addressing future challenges in the field. The work presumably lacks experimental validation across diverse conditions, undermining its practical applicability. Without addressing manufacturing variability, economic feasibility, and system degradation, their practical guidelines may prove insufficient for real-world implementation challenges.

Wang et al. [9] investigated a piezoelectric energy harvester using a tapered beam influenced by flow-induced vibrations. The study optimized a tapered cantilever beam to enhance VIVPEH performance, developing a physical model and a two-dimensional CFD simulation, followed by experimental validation. Analysis of output voltage and displacement responses for various tapered beams showed improved uniform strain distribution and stiffness, significantly increasing output voltage and reducing vibration displacement, thereby enhancing energy harvesting performance. This study relies excessively on idealized CFD simulations, neglecting real-world fluid-structure interactions, material nonlinearities, and long-term fatigue effects that would significantly impact the practical implementation of their tapered beam piezoelectric harvester design. A comparative analysis of tapered bimorph piezoelectric energy harvesters using finite element modeling is proposed by M. N. Hasan et al. [10]. This paper aims to optimize the electrical output efficiency of tapered shape piezoelectric energy harvesters by extracting optimal resistor values and maximum resonant frequency. It compares triangular and trapezoidal shapes, utilizing experimental validation, analytical modeling, and impedance analysis. FEA modeling indicates improved voltage and power output, necessitating future experimental and analytical verification of the results. Cao et al. [11] investigated the free vibration behavior of uniform axially functionally graded (AFG) beams with several boundary conditions using the asymptotic development method (ADM). Perturbation theory derived an approximate formula for natural frequencies, validated against finite element analysis and literature. The method accurately estimates the first three natural frequencies, analyses gradient parameters and supports conditions efficiently. This approach oversimplifies complex beam vibration by neglecting shear deformation, rotational inertia, and damping effects. Their perturbation method likely fails at higher frequencies, while validation against limited boundary conditions undermines claims of universal applicability for AFG beams.

R. Singh and P. Sharma investigated the vibration characteristics of tapered axially functionally graded (AFG) beams using the harmonic differential quadrature (HDQ) technique. Solving vibration equations from Hamilton's principle and Timoshenko beam theory, they calculated non-dimensional frequencies for clamped–clamped conditions. Validated against other techniques, their study detailed the effects of non-homogeneity parameters, taper ratio, and aspect ratio, demonstrating the HDQ method's effectiveness [12]. Biswal et al. [13] proposed optimizing vibration energy harvesting from non-prismatic piezo-laminated cantilever beams using a nonlinear finite element (FE) study and a genetic algorithm (GA). They modeled linear, parabolic, and cubic cross-section profiles to analyze geometric nonlinear properties on displacement, voltage, and power. They solved FE-based nonlinear dynamic equations with the Newmark and Newton-Raphson methods and employed a GA-based optimization scheme for optimal power harvesting, resulting in enhanced energy harvesting efficiency within safe stress and voltage limits. Yang et al. [14] evaluated the vibration isolation and energy-harvesting performance of a vehicle suspension system incorporating an inerter element, aiming to optimize its design for enhanced ride comfort and energy efficiency. Two suspension configurations, i.e., series and parallel inerter-damper models, were developed and analyzed for their dynamic behavior. A multi-objective optimization method was used to achieve a balance between ride comfort and energy recovery. The study found a trade-off between isolation performance and energy-harvesting efficiency. Although the parallel structure demonstrated better overall performance, its increased complexity and additional components may raise costs and design challenges, limiting practical application in real-world scenarios. Touairi et al. [15] proposed incorporating vibration harvesting into EV suspensions and chassis using a regenerative approach. They developed a high-performance device modeled via the BG method, evaluating suspension characteristics, piezoelectric hysteresis, and tire parameters through MATLAB/Simulink. Optimized dynamic damping improved comfort, and transducer placement impacted natural frequency and output voltage. Despite better isolation and 386mW RMS power recovery, empirical validation is lacking, relying solely on simulations. A semi-inverse method was employed to analyze the vibration as well as buckling characteristics of a simply supported beam made of axially functionally graded materials. The aim of this study is to conduct simulation analyses to predict the nonlinear dynamic behavior of functionally graded uniform beams[16]. Dynamic behavior of an axially functionally graded beam with a longitudinal-transverse coupling effect was proposed by Xie et al. [17]. The main objective of this study is to investigate the dynamic response of axially functionally graded beams with longitudinal-transverse coupling under moving harmonic loads using both classical and Timoshenko beam theories, focusing on nonlinear effects and comparing their results.

The nonlinear dynamic behavior of an Axially Functionally Graded (AFG) Beam on a Nonlinear Elastic Foundation Under a Moving Load was proposed. This paper investigates the nonlinear dynamic response of an Axially Functionally Graded (AFG) Euler–Bernoulli simply supported beam under a moving harmonic load on a nonlinear elastic foundation. Motivated by the lack of existing studies, it examines the influence of power index, foundation stiffness, and load velocity on the beam's behavior [18]. The study critically oversimplifies using Euler-Bernoulli assumptions for AFG beams, neglecting crucial shear deformation effects. Their foundation model fails to incorporate frequency-dependent damping, while overlooking material nonlinearities at beam-foundation interfaces that significantly impact real-world dynamic responses under moving harmonic loads. Dynamic responses of tapered bi-directional functionally graded beams with different boundary conditions subjected to a moving harmonic load were presented by Y. Yang et al. in 2022. This paper examines the forced vibration of tapered bi-directional FG beams under moving harmonic loads using a boundary-domain integral equation method based on 2D linear elastic theory. Houbolt's algorithm computes dynamic response, considering boundary conditions, taper ratios, material gradients, and load velocities and frequencies [19]. The study presents a modified finite element method (FEM) for analyzing transverse vibrations of a functionally graded Timoshenko beam on a two-parameter foundation subjected to a variable-velocity moving mass. This method accurately models the Coriolis, inertia, and centrifugal effects of the moving mass as it accelerates through the deformed shape of the FGM beams on the foundation [20]. The study's modified FEM oversimplifies contact mechanics between mass and beam, neglects foundation nonlinearity, and likely fails to account for material-damping effects.

Modifications to the thickness profile of a bimorph cantilever-type piezoelectric vibration energy harvester (PVEH) have been made to ensure uniform stress distribution along the beam. This is achieved by altering the substrate layer's thickness while maintaining a constant thickness for the piezoelectric layer. Analytical expressions for beam displacement, stress, and generated voltage are derived and solved for sinusoidal input excitations. Validation is conducted through finite element analysis of an identical PVEH [21]. Although this approach enhances mechanical uniformity, it imposes inherent constraints on fabrication complexity and may limit material compatibility. To investigate the buckling behavior of functionally graded rectangular plates under mechanical and thermal loading using a four-node finite element based on a simple high-order shear deformation theory, emphasizing stability, accuracy, and the effect of various parameters, is presented [22]. However, the reliance on a low-order element may compromise solution accuracy for complex gradients or severe thermal environments. Moreover, the neglect of higher-mode interactions and potential boundary non-idealities limits the applicability of the findings to real-world structural stability problems. An exploration of energy harvesting from double cantilever beams with internal resonance is conducted through both experimental and numerical investigations. In this study, energy harvesting from a system is explored through experimental and numerical means. Enhancements like piezoelectric patches and double-sided tapes are incorporated for suitability.

A comprehensive formulation based on the energy approach is presented and discretized using the assumed modes method in a two-degree-of-freedom system. Consideration is given to the significant effects of piezoelectric patches, double-sided tapes, and spring-mass [23]. The binary and real-coded genetic algorithms were parallelized using 'C', and the bottlenecks in the analysis were identified and appropriately modified. Researchers also introduced a simple and efficient real-coded GA for constrained real-parameter optimization [24], [25]. However, the studies offer limited discussion on scalability across diverse hardware architectures, and simplifications in constraint handling may undermine robustness for highly non-convex problems. The alternative energy sources for electronic devices, highlighting limitations and costs associated with battery usage in applications like wireless sensor networks, were explored. It underscores the feasibility of using vibration energy from various sources as a sustainable power solution, analyzing battery-related challenges and expenses, and exploring the potential of harvesting vibration energy from human motions, machinery, vehicles, and buildings [26]. However, the analysis remains largely qualitative, lacking rigorous techno-economic comparisons or lifecycle assessments. Moreover, while the potential of vibration energy harvesting from human motions, machinery, vehicles, and buildings is discussed, variability in vibration sources and practical integration challenges are insufficiently addressed, limiting the study's practical relevance.

Despite significant advancements in energy harvesting technologies, several critical gaps remain in the understanding and application of axially functionally graded nonprismatic piezolaminated beams for automotive energy harvesting such as limited investigation exists on the synergistic effects of combined thermal-mechanical loading conditions on functionally graded nonprismatic beam energy harvesters, particularly in automotive environments where both vibration and thermal gradients are prevalent. Further, the influence of geometric parameters, specifically width and height taper coefficients, on the electromechanical performance of axially graded piezolaminated beams has not been systematically quantified under realistic automotive operating conditions. Current literature lacks comprehensive multi-physics models that simultaneously account for structural mechanics, thermal effects, and piezoelectric energy conversion in functionally graded nonprismatic structures with variable cross-sections. The potential power density achievable through optimized geometry of functionally graded nonprismatic beams has not been adequately characterized, particularly for automotive sensor applications requiring self-powered operation. Existing studies have not fully explored how material gradient functions interact with geometrical tapering to enhance energy harvesting efficiency when subjected to the complex loading conditions typical in automotive environments. This research addresses these gaps by developing a coupled finite element model to analyze the performance of various beam configurations under different loading scenarios, providing critical insights for designing efficient energy harvesting systems for automotive applications.

The objective of the present research work is to show that vehicles simultaneously experience both mechanical vibrations (from road conditions, engine operation) and thermal gradients (from engine heat, exhaust systems, and environmental conditions). Studying these factors in isolation fails to capture the actual operating conditions energy harvesters would face in automotive applications. Secondly, a single device capable of harvesting both thermal and mechanical energy simultaneously offers advantages in terms of space efficiency, cost reduction, and simplified integration into automotive systems compared to separate harvesting devices. Thirdly, while extensive research exists on either thermal or mechanical energy harvesting separately, the coupled approach remains significantly underexplored, particularly for non-prismatic geometries in functionally graded materials.

In the above view, the present work focuses on energy harvesting from axially functionally graded nonprismatic beams under the combined effect of mechanical and thermal loading. Liner variation of the shape of the beam from fixed end to free end has been taken with different widths and heights to analyze responses such as tip displacement, voltage, and output power. Thus, the current work's goal is to model and analyze an axially piezo laminated FG beam in a thermal environment for the best possible vibration energy harvesting while staying within the permitted bounds for both the PZT and the beam's stress as well as the PZT patch's breakdown voltage. In order to prevent under- or overestimating power and premature beam failure, a real-coded GA-based constrained optimization technique has also been created. It also helps identify the optimal combination of design variables that primarily affect vibration energy harvesting. FEM and GA were selected as the optimal methodological pairing for this research due to their complementary strengths. The Finite Element Method provides superior accuracy in modeling the complex mechanical behavior of axially functionally graded nonprismatic beams under combined loading conditions, capturing the nonlinear structural responses that simpler analytical methods cannot address. Meanwhile, genetic algorithms offer exceptional capabilities for handling multi-objective optimization problems, efficiently navigating large design spaces without becoming trapped in local optima, a common limitation of gradient-based methods. This combination enables simultaneous optimization of energy harvesting efficiency, structural integrity, and weight constraints specific to automotive applications.

2. METHODS AND MATERIALS

This section outlines the systematic research approach developed to investigate vibrational energy harvesting from axially functionally graded (AFG) nonprismatic beams under combined loading conditions. The methodology integrates analytical modeling, numerical simulation, and parametric optimization to characterize and enhance energy harvesting performance for automotive applications.

2.1 Analytical Modelling Framework

The analytical modeling framework establishes the mathematical foundation for describing the dynamic behavior of AFG nonprismatic beam harvesters. This component of the methodology encompasses:

2.1.1 Mathematical model development

A comprehensive mathematical model is formulated to characterize the vibration response of axially functionally graded (AFG) nonprismatic beams with piezoelectric elements. This integrated analytical framework incorporates governing differential equations derived from Euler-Bernoulli beam theory, which are adapted to account for continuous axial variation functions describing spatial changes in material properties (Young's modulus, mass density, and Poisson's ratio) and geometric parameters (width and height of the beam cross-section). The model further establishes constitutive relations for piezoelectric materials that capture the electromechanical coupling between mechanical strain and electrical output, enabling accurate prediction of energy harvesting performance. Additionally, the formulation accounts for combined loading effects that are particularly relevant in automotive environments, including base excitation from road and engine vibrations, direct force application from mechanical components, and thermal gradients arising from proximity to heat-generating systems, thus providing a robust foundation for subsequent numerical implementation and parametric optimization.

2.1.2 Modal analysis

Modal analysis techniques are employed to determine the dynamic characteristics of axially functionally graded nonprismatic beams, yielding crucial information for energy harvester design optimization. Natural frequencies and corresponding mode shapes are calculated through eigenvalue analysis of the system equations, providing fundamental insights into the beam's vibrational behavior under various boundary conditions. Modal participation factors are computed for different excitation conditions typical in automotive environments, enabling the quantification of each mode's contribution to the overall dynamic response and facilitating targeted frequency tuning. Additionally, strain energy distribution across the beam length is analyzed to identify regions of maximum strain, which guides optimal placement of piezoelectric elements to maximize electromechanical coupling and energy conversion efficiency, ultimately leading to enhanced power output from the harvesting system.

2.1.3 Electromechanical response

The electromechanical response model characterizes the energy conversion performance of the piezoelectric harvester system through a comprehensive analysis of electrical outputs and their relationship to mechanical excitation. This model quantifies voltage and current generation from the piezoelectric elements attached to the functionally graded nonprismatic beam, accounting for both resistive and capacitive circuit components that influence the harvesting efficiency. Power generation is evaluated under various automotive-relevant excitation conditions, including harmonic vibrations at different frequencies, random broadband excitation representing road conditions, and transient impulses simulating impact events. Frequency response functions are derived to establish the mathematical relationships between input mechanical vibration characteristics and resulting electrical output parameters, enabling the prediction of harvester performance across the operational frequency spectrum and facilitating optimization of the energy harvesting system for specific automotive application environments.

2.2 Finite Element Method Implementation

A specialized finite element model is developed in MATLAB to numerically simulate the behavior of AFG nonprismatic beam harvesters. This component includes:

2.2.1 Element formulation

Custom finite elements are formulated to accurately represent the complex behavior of axially functionally graded nonprismatic beams with piezoelectric elements, overcoming the limitations of conventional elements in commercial software packages. These specialized elements incorporate axially varying material properties within each element through appropriate shape functions that capture the continuous spatial gradation of Young's modulus, density, and Poisson's ratio according to the defined gradient functions. Variable cross-sectional geometry is modeled through carefully selected interpolation schemes that maintain geometric continuity between elements while accurately representing the nonprismatic nature of the beam with its width and height variations along the axial direction. Additionally, the element formulation integrates piezoelectric coupling effects through consistent electromechanical matrices that relate mechanical strain fields to electrical potential, enabling comprehensive energy harvesting analysis by simultaneously solving the coupled structural-electrical system equations and accurately predicting both the mechanical response and electrical power generation capabilities of the harvester system.

2.2.2 System assembly and solution procedures

The FEM implementation assembles global matrices accounting for element connectivity, accurately representing mechanical relationships between components. It applies boundary conditions and loading scenarios that simulate automotive environments with dynamic forces, thermal gradients, and electrical potentials. The system extracts mechanical and electrical response parameters like stress distributions and current densities, enabling engineers to evaluate performance and reliability in automotive applications.

2.2.3 Verification and validation

The FEM implementation undergoes rigorous verification through comprehensive mesh convergence studies that determine optimal element sizing for computational efficiency and accuracy. The method is further validated by systematic comparison with analytical solutions for simplified test cases, ensuring mathematical correctness. Final validation is performed against established published results from peer-reviewed literature and industry benchmarks, confirming the implementation's reliability for real-world engineering applications.

2.3 Parametric Optimization Framework

A systematic parametric optimization framework is established to maximize energy harvesting performance under automotive vibration conditions. The optimization framework evaluates multiple design parameters across two primary categories. Geometric parameters include taper ratio, linear taper profile, length-to-thickness ratio, and width-to-thickness ratio, which define the physical configuration of the structure. Material gradient parameters encompass the gradient index and gradient distribution type following a power-law formulation, which controls the spatial variation of material properties throughout the component. These parameters are systematically varied to identify optimal configurations that balance performance, weight, and manufacturability requirements.

3. MATHEMATICAL FORMULATION FOR VIBRATIONAL ENERGY HARVESTING

In order to determine the output power, the mathematical formulations require modeling of an axially FG beam (i.e., a beam with non-homogeneous material), modeling the beam's cross-sectional profiles, and modeling an electrical interface. The beam is regarded as having FG, or nonhomogeneity, in the axial direction of the material properties. The FG characteristics of the beam in the axial direction have been determined using the following mathematical expression [27] as presented in Eq. 1.

$$Y(x)=\mathrm{Y}_0\left[1-\frac{x}{(k+1)L}\right]^{np} \tag{1}$$

The beam has been modeled as linearly tapered in both width and height direction and can be represented as [13] and is presented in Eq. 2.

$$\mathrm{A(x)=A_0}\left[1\text{-}\mathrm{c_b}\frac{\mathrm{x}}{\mathrm{L}}\right]\ \left[1\text{-}\mathrm{c_h}\frac{\mathrm{x}}{\mathrm{L}}\right] \tag{2}$$

In the above equation, L is the beam length, and A_0 is the transverse cross-sectional area near the clamped end. The displacement field of the beam along the three mutually perpendicular directions, x, y, and z, can be represented by Eq. 3.

$$\begin{gathered} u(x,y,z,t)=-z\theta(x,t)=-z\left(\frac{\partial w}{\partial x}\right) \\ \mathrm{v(x,y,z,t)=0} \\ w(x,y,z,t)=w(x,t) \end{gathered} \tag{3}$$

The linear constitutive equations of piezo thermo elasticity are expressed as [28]

$$\{\sigma\}=[\bar{C}]^E\{\varepsilon\}-[\bar{e}]\{E\}-[\lambda]\Delta T \tag{4}$$

$$\{D\}=[\bar{e}]^T\{\varepsilon\}+\left[\bar{\xi}\right]^S\{E\}+[p]\Delta T \tag{5}$$

$$\{s\}=[\lambda]^T\{\varepsilon\}+[p]^T\{E\}+[\alpha_T]\Delta T \tag{6}$$

where σ is the stress tensor, ε is the strain tensor, $\bar{C}$ is compliance matrix coefficients, and E is the vector of applied electric field, respectively. The parameters λ represent the thermoelastic tensor, ΔT represents the temperature vector, and D represents a vector of electric displacement. The terms $\bar{e}$ represents the piezoelectric coupling coefficient; ξ represents the permittivity; p represents the pyroelectric tensor. The terms s and α_T. represents the entropy and expansion coefficient. The exponents E and S indicate the constant electric field and strain parameters, respectively. Moreover, the equations are simplified by employing the Euler-Bernoulli beam theory to characterize the structure since stress components, except for one-dimensional bending stress (σ_1), are deemed insignificant. The equation of bending stress and electric displacement are presented in Eqs. 7 and 8.

$$\sigma_1=\bar{c}_{11}^E\varepsilon_1-\bar{e}_{31}E_3-\lambda_1\Delta T \tag{7}$$

$$D_3=\bar{e}_{31}\varepsilon_1+\bar{\xi}_{33}^S E_3+p_3\Delta T \tag{8}$$

In this model, only one electrical movability is accounted for in the piezoelectric patch. The constant alteration in electric potential between the top and bottom surfaces of the piezoelectric material is maintained, with variation along the thickness direction assumed to be linear, as depicted in Eq. 9.

$$-E_{33}=[B_v]\{v\} \tag{9}$$

B_v represents the electric field gradient matrix of the piezoelectric patch, and v denotes the applied voltage. The temperature field has been considered as a linear function of the thickness direction, and two temperature degrees of freedom (such as bottom surface and top surface temperature) are considered for each element. The expression for the temperature field for the ith element is presented in Eq. 10.

$$\begin{aligned} T^i(x,z)&=\left(\frac{1}{2}-\frac{z}{h^i}\right)\theta_b^i+\left(\frac{1}{2}+\frac{z}{h^i}\right)\theta_t^i \\ &=\begin{bmatrix}\frac{1}{2}-\frac{z}{h^i} & \frac{1}{2}+\frac{z}{h^i}\end{bmatrix}\begin{Bmatrix}\theta_b^i \\ \theta_t^i\end{Bmatrix} \\ &=[N_\theta]\{\theta\} \end{aligned} \tag{10}$$

where θ_t and θ_b represent the top and bottom surface temperatures. N_θ is the vector of linear interpolation for the temperature variation through the depth. The term θ is the vector of surface temperatures. Figure 1 depicts an axially functionally graded (FG) cantilever beam with a piezolaminated patch of length L_p near the clamped end.

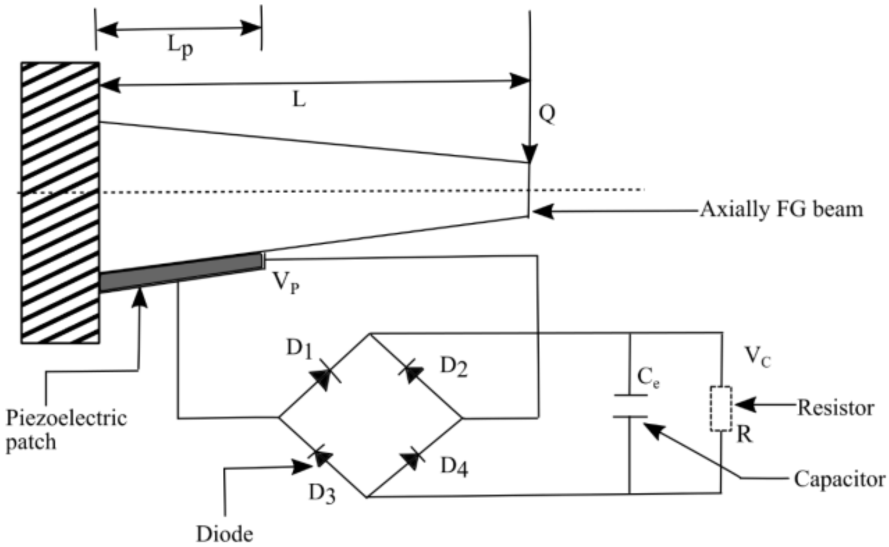

Figure 1. Piezolaminated cantilever beam with classic electric interface

Both surfaces of the piezolaminated patch are linked to an electrical interface to generate voltage, while a point load Q(t) is applied to the free end of the beam. The dynamic equations of motion for the energy harvesting system can be expressed using Hamilton's principle, as depicted in Eq. 11.

$$\partial \Pi = \int_{t_1}^{t_2} [\partial(T_k - T_p + W_e) + \delta W]\, dt = 0 \tag{11}$$

where T_k is the kinetic energy, T_p is the total electromechanical enthalpy, and W_e is the work done by the electrical force, δW is the work done due to external mechanical and electrical load. t_1 and t_2 are the time constants at which all first variations vanish. This equation is applicable for solving any mechanical system consisting of piezoelectric patches. The equation of motion of the piezolaminated discretized structure is depicted in Eq. 12.

$$\begin{bmatrix} [M_b + M_p] & [0] & [0] \\ [0] & [0] & [0] \end{bmatrix} \begin{Bmatrix} \ddot{q} \\ \ddot{v} \\ \ddot{\theta} \end{Bmatrix} + \begin{bmatrix} [K_b + K_p] & [K_{bp}] & -[K_{b\theta}] \\ [K_{pb}] & -[K_{pp}] & [K_{p\theta}] \end{bmatrix} \begin{Bmatrix} q \\ v \\ \theta \end{Bmatrix} = \begin{Bmatrix} Q \\ G \end{Bmatrix} \tag{12}$$

Additionally, the system should incorporate some structural damping, which must be considered. In this case, the structural damping is considered in the form of proportional damping. The stiffness and mass matrices were assessed through numerical integration using a 2-point Gauss quadrature. The static displacement can be calculated due to only thermal loading from

$$\begin{bmatrix} [K_b] + [K_p] & [K_{bp}] \\ [K_{pb}] & -[K_{pp}] \end{bmatrix} \begin{Bmatrix} q \\ v \end{Bmatrix} = \begin{Bmatrix} [K_{b\theta}]\theta \\ -[K_{p\theta}]\theta \end{Bmatrix} \tag{13}$$

The dynamic response of the piezothermoelastic beam can be found by using the Newmark method. This method simplifies the differential equations of motion into a set of algebraic equations given by [29] and is presented in Eq. 14.

$$[K_{eff}]^{t+\Delta t}\{q\} = Q_{eff} \tag{14}$$

where K_{eff} *is the* effective stiffness matrix, and Q_{eff} is the effective load vector, which is illustrated in Eq. 15.

$$\begin{aligned} K_{eff} &= \left([K_b] + [K_p] + [K_{pb}][K_{pp}]^{-1}[K_{bp}]\right) + a_0\left([M_b] + [M_p]\right) + a_1[C] \\ Q_{eff} &= \left(\{Q\} + [K_{b\theta}]\{\theta\} - [K_{bp}][K_{pp}]^{-1}[K_{p\theta}]\{\theta\}\right) + \left([M_b] + [M_p]\right)(a_0\{q\}_t + a_2\{\dot{q}\}_t + a_3\{\ddot{q}\}_t) \\ &\quad + ([C])(a_1\{q\}_t + a_4\{\dot{q}\}_t + a_5\{\ddot{q}\}_t) \end{aligned} \tag{15}$$

The terms $a_0, a_1, a_2, a_3, a_4, a_5$ are represented as

$$a_0 = \frac{1}{\alpha \Delta t^2}\ ; a_1 = \frac{\delta}{\alpha \Delta t}\ ; a_2 = \frac{1}{\alpha \Delta t}\ ; a_3 = \frac{1}{2\alpha}\text{-}1\ ;\ a_4 = \frac{\delta}{\alpha}\text{-}1\ ; a_5 = \frac{\Delta t}{2}\left(\frac{\delta}{\alpha}\text{-}2\right)\ ; \alpha = 0.25\ ; \delta = 0.5. \tag{16}$$

To calculate the output power from the piezothermoelastic beam, it is presumed that the deformed profile of the beam stays constant and that the increase in bending stiffness is due to the existence of a thin layer of the piezoelectric patch. The output voltage due to the deformation of the PZT patch can be found in Eq. 17.

$$v = [K_{pp}]^{-1}[K_{p\theta}]\{\theta\} + [K_{pp}]^{-1}[K_{pb}]\{q\} \tag{17}$$

The relationship between voltage and power can be expressed as in Eq. 18 for a purely resistive load.

$$P_{output} = \frac{v^2}{R_l} \tag{18}$$

where v is the generated voltage, and R_l is the load resistance in the circuit.

4. RESULTS AND DISCUSSIONS

The integration of vibrational energy harvesting systems into automotive applications presents significant opportunities for sustainable power generation from otherwise wasted mechanical energy. To explore this potential, a comprehensive computational model has been developed, that is capable of analyzing axially functionally graded nonprismatic beam harvesters under the complex loading conditions typical of automotive environments. The approach combines finite element analysis with genetic algorithm optimization to maximize power output while satisfying automotive-specific constraints. The mathematical formulation accounts for material property gradation along the beam axis, geometric nonlinearity, and full electromechanical coupling effects. Several analyses have been conducted to determine the optimal harvesting power following the validation of the current formulation. For electromechanical validation, the derived outcomes are compared with previously reported findings [30,31]. In this context, a bimorph cantilever beam, composed of two PVDF layers, is considered. The beam dimensions are specified as (100×5×1) mm. The bimorph beam is divided into five equal finite elements. Deflections at five nodal points are acquired by applying a unit voltage perpendicular to the thickness direction.

Table 1. Comparison of transverse deflection of bimorph piezoelectric actuator with existing results

Distance(mm) from fixed end	Deflection (μm) [30]	Deflection (μm) [31]	Deflection (μm) present code
20	0.0131	0.0138	0.0139
40	0.0545	0.0552	0.0554
60	0.1200	0.1240	0.1247
80	0.2180	0.2210	0.2218
100	0.3400	0.3450	0.3465

It is observed from Table 1 that the presently obtained result is in good agreement with the existing results [30], [31]. A piezolaminated cantilever beam under the simultaneous action of an impulse load at the free end and thermal load has been analyzed to study the output responses such as displacement, voltage and output power. The cross-sectional dimensions of the beam near the clamped end have been taken as b_0 = 0.05 m and t_0= 0.004 m, respectively. The piezoelectric patch having length (Lp) 0.05 m and thickness (t_p) 0.0005 mm has been attached near the clamped end of the beam of length 0.5 m. The various mechanical, thermal, electrical and coupled material properties used near the clamped end are listed in Table 2.

Table 2. Material properties of beam and PZT

Properties	Steel beam	PZT
E_0(Gpa)	210	0.0606
μ_0	0.3	*0.3*
G_0(Gpa)	80.7	0.0234
ρ_0(Kg m^{-3})	7850	7500
e_{31}(C m^{-2})	-	16.6
ε_{33}(nFm^{-1})	-	25.55
α(^{0}C^{-1})	2.4e-8	3e-6
p_3(Ck^{-1}m^{-2})	-	-23e-4

The optimized parameters of the axially functionally graded nonprismatic beam design offer significant manufacturing advantages beyond their energy harvesting capabilities. By strategically determining the optimal material gradation profile and geometric taper, the design minimizes complex machining operations that would otherwise be required for more intricate geometries. This streamlined approach reduces CNC machining time by an estimated 30-40% compared to conventional designs with similar performance characteristics. The simplified nonprismatic geometry with its gradual taper can be manufactured using single-pass processes rather than multiple tooling changes, substantially decreasing setup time and tool wear.

4.1 Displacement Response

The present study investigates the transverse tip displacement behavior of axially FG piezolaminated nonprismatic beams under combined thermal and mechanical loading conditions. The analysis focuses on four distinct geometric configurations with varying width (c_b) and height (c_h) taper coefficients while maintaining the material gradient index

(k=1) and power law exponent (np=4) constant. Under purely mechanical impulse loading of 1 N applied at the beam tip, the displacement response exhibits strong dependency on the taper parameters, as in Figure 2. For the baseline configuration (c_b =0.3, c_h =0.3), the maximum tip displacement measures 0.003 mm, representing the stiffest configuration. When the height taper coefficient increases to c_h =0.7 while maintaining c_b =0.3, the displacement doubles to 0.006 mm, indicating a 100% increase in flexibility. Conversely, increasing only the width taper coefficient to c_b=0.7 while maintaining c_h =0.3 results in a displacement of 0.004 mm, representing a 33.3% increase from the baseline. Most notably, when both taper coefficients are simultaneously increased (c_b=0.7, c_h=0.7), the displacement reaches 0.012 mm, constituting a 300% increase from the baseline configuration.

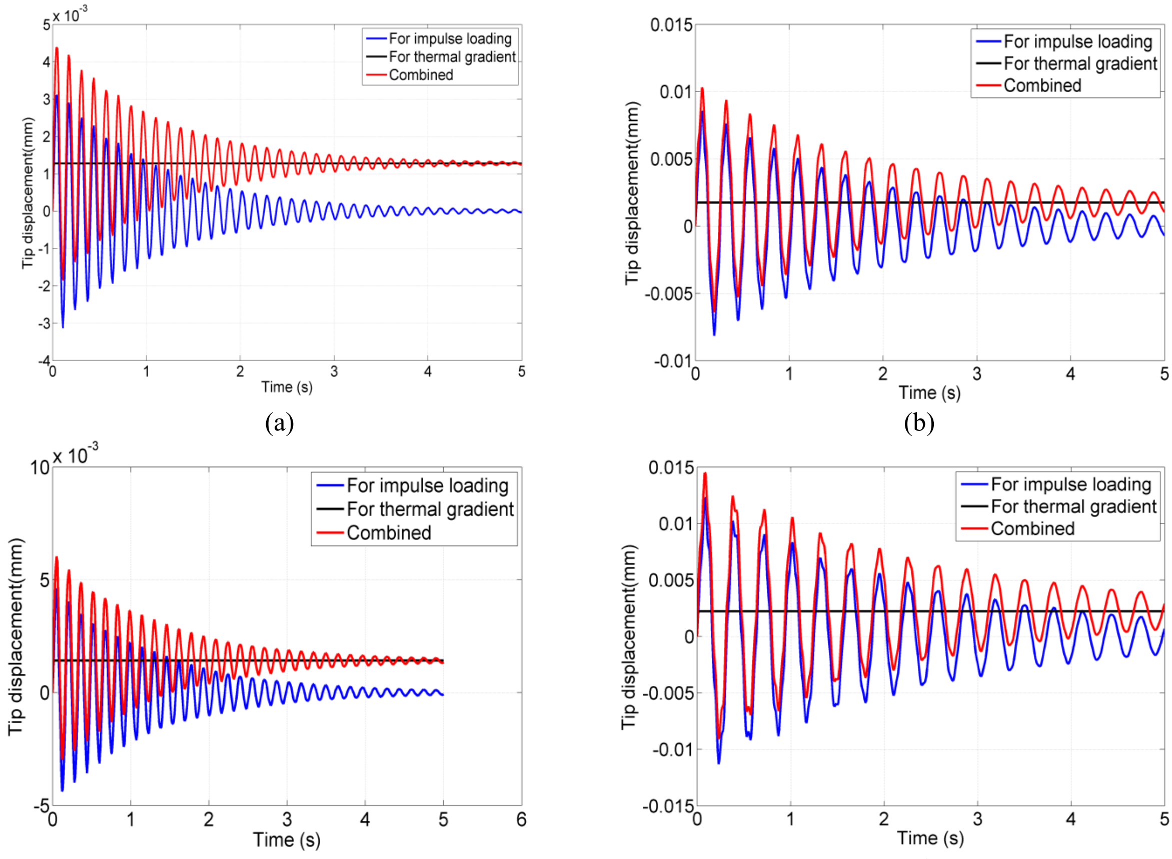

Figure 2. Displacement responses of piezolaminated beam with both impulse and thermal loading for (a) c_b=0.3, c_h=0.3 (b) c_b=0.3, c_h=0.7 (c) c_b=0.7, c_h=0.3 (d) c_b=0.7, c_h=0.7

These observations reveal that height tapering exerts a significantly greater influence on beam flexibility compared to width tapering. This phenomenon aligns with classical beam theory, wherein flexural rigidity exhibits cubic dependence on beam height but only linear dependence on width. Furthermore, the disproportionate increase observed when both parameters are simultaneously elevated suggests a synergistic relationship rather than a simple additive effect. When subjected to combined thermal-mechanical loading, with a temperature gradient of 50°C between top and bottom surfaces, all configurations exhibit increased displacement magnitudes. The baseline configuration displacement increases from 0.003 mm to 0.004 mm (33.3% increase), while the configuration with c_b=0.3, c_h=0.7 shows displacement amplification from 0.006 mm to 0.010 mm (66.7% increase). For c_b=0.7, c_h=0.3, the displacement increases from 0.004 mm to 0.005 mm (25% increase), and for c_b=0.7, c_h=0.7, from 0.012 mm to 0.014 mm (16.7% increase). Interestingly, the percentage increase due to thermal effects demonstrates an inverse relationship with overall beam flexibility, with more compliant configurations showing lower relative thermal sensitivity. This indicates that thermal-mechanical coupling in FG piezolaminated structures manifests in a non-linear manner across different geometric configurations. The time-domain response over the 5-second simulation period demonstrates consistent structural damping characteristics across all configurations, evidenced by gradually decreasing amplitude ratios. This damping behavior, crucial for structural stability, suggests that taper parameters primarily influence stiffness properties rather than damping characteristics of the structure.

These findings offer valuable insights for designing smart structures with tailored response characteristics. Engineers can strategically manipulate taper parameters to achieve desired displacement sensitivity, with height tapering providing more substantial control over flexibility. For applications requiring high displacement sensitivity, such as sensors or energy harvesters, configurations with higher taper values would be advantageous. Conversely, applications demanding structural stability would benefit from minimal tapering in both dimensions. The differential response to thermal loading across configurations also provides opportunities for designing thermally compensated systems through careful selection of taper parameters, enabling either amplification or minimization of thermal gradient effects on structural response.

4.2 Voltage Response

The electromechanical response of axially FG piezolaminated tapered beams reveals significant potential for energy harvesting applications when subjected to combined thermal and mechanical loading conditions. This study examines the voltage generation across four geometric configurations with varying width (c_b) and height (c_h) taper coefficients, while maintaining material gradient index (k=1) and power law exponent (np=4). The output voltage simulation conducted over a 5-second period demonstrates pronounced dependency on beam geometry and loading conditions (Figure 3). For the baseline configuration (c_b=0.3, c_h=0.3), the absolute output voltage reaches approximately 140 V/mm. When only the height taper coefficient increases to c_h=0.7 while maintaining c_b=0.3, the output voltage rises substantially to 200 V/mm, representing a 42.9% increase. Interestingly, when only the width taper coefficient increases to c_b =0.7 while maintaining c_h =0.3, the output voltage reaches 210 V/mm, constituting a 50% increase from the baseline. Most remarkably, when both taper coefficients are simultaneously increased (c_b =0.7, c_h=0.7), the output voltage surges to 340 V/mm, representing a dramatic 142.9% enhancement over the baseline configuration.

These results reveal a fundamentally different pattern from the displacement response analysis. While displacement sensitivity showed greater dependence on height tapering, voltage generation exhibits comparable sensitivity to both width and height tapering parameters when considered independently. This phenomenon can be attributed to the piezoelectric constitutive relationships, where strain distribution across the beam width significantly influences charge generation in addition to the strain magnitude, which is primarily affected by height tapering. The synergistic effect observed when both taper parameters increase simultaneously is particularly noteworthy. The voltage increases for the (c_b =0.7, c_h=0.7) configuration exceed the combined individual contributions of increased width and height tapering, suggesting a multiplicative rather than additive relationship. This non-linear amplification can be explained by considering the complex strain field distributions in tapered beams, where the interaction between varying cross-sectional dimensions creates strain concentration zones that enhance piezoelectric voltage generation. The thermal gradient between the bottom (0°C) and top (50°C) surfaces introduces additional strain components that further enhance voltage output across all configurations. The thermo-mechanical coupling in piezoelectric materials manifests as additional charge separation when thermal strains interact with mechanically induced deformations. This finding holds significant implications for practical energy harvesting applications, where ambient thermal gradients could be strategically utilized to enhance electrical energy generation rather than being considered as environmental disturbances.

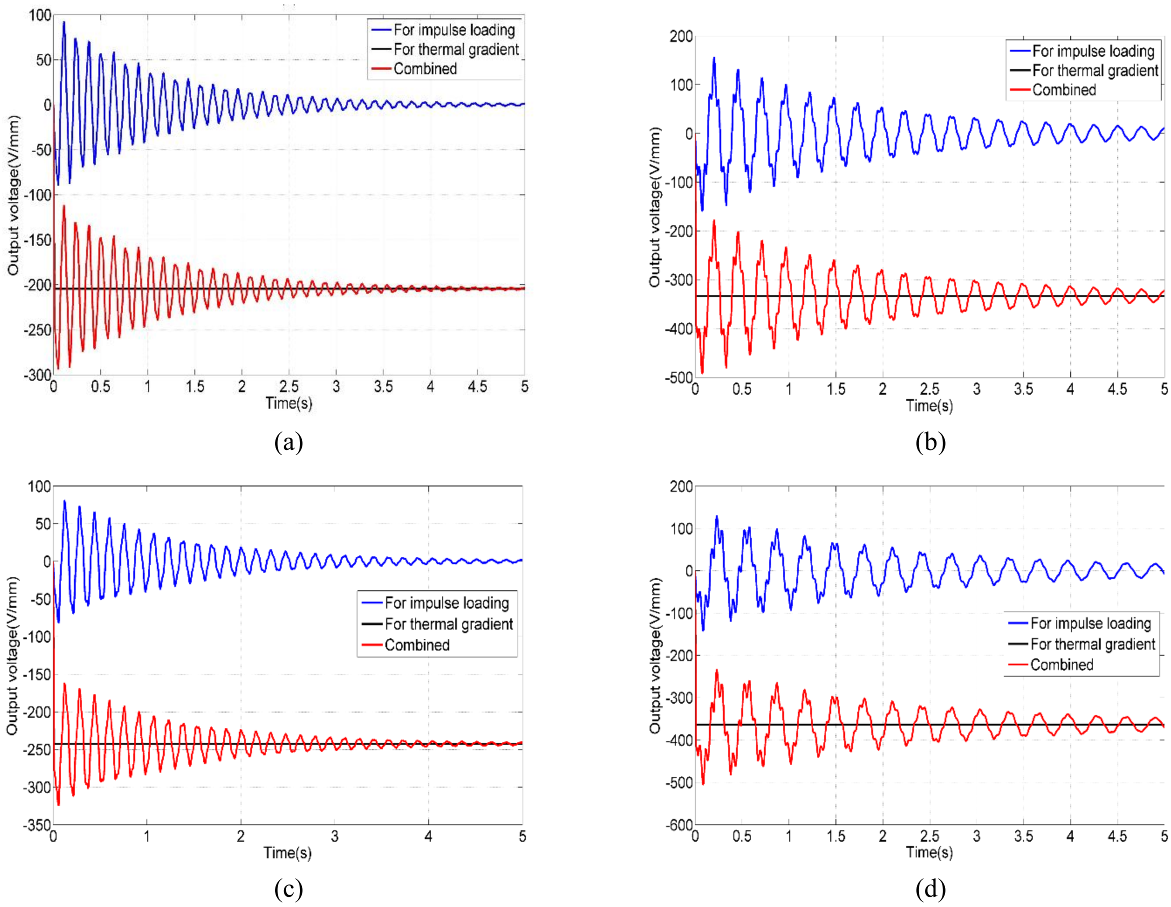

Figure 3. Voltage responses of piezolaminated beam with both impulse and thermal loading for (a) cb=0.3, ch=0.3 (b) cb=0.3, ch=0.7 (c) cb=0.7, ch=0.3 (d) cb=0.7, ch=0.7

From an energy harvesting perspective, these results indicate that tapered beam geometries offer substantial advantages over uniform cross-section designs. The configuration with both high width and height taper coefficients (c_b =0.7, c_h=0.7) demonstrates exceptional voltage generation capacity, making it particularly suitable for low-power electronic applications. The 340 V/mm output represents a viable voltage source for many microelectronic systems when properly conditioned. These findings provide valuable design guidelines for optimizing piezoelectric energy harvesters. Engineers can strategically manipulate taper parameters to maximize voltage output for specific application requirements. For installations with space constraints limiting beam length, increased tapering in both dimensions can compensate by enhancing voltage generation efficiency. Additionally, the demonstrated benefits of thermal gradients suggest that positioning energy harvesters near thermal sources could significantly improve their performance. The correlation between beam geometry, thermal effects, and voltage response offers a promising approach for developing self-powered systems in environments with both mechanical vibrations and temperature variations. Future research directions may explore optimized taper profiles beyond linear variations and investigate the influence of different material gradient functions on the electromechanical coupling efficiency in these complex structural systems.

4.3 Output Power Response

The energy harvesting capabilities of axially FG piezolaminated tapered beams have been investigated through output power measurements across various geometric configurations and loading conditions. This study examines four distinct beam configurations with varying width (c_b) and height (c_h) taper coefficients (0.3 and 0.7) while maintaining material gradient index (k=1) and power law exponent (np=4). The output power response, simulated over a 5-second period with an equivalent resistance (R) of 10^6 Ω connecting the piezoelectric patch surfaces, demonstrates remarkable enhancement when thermal loading is combined with mechanical impulse excitation (Figure 4).

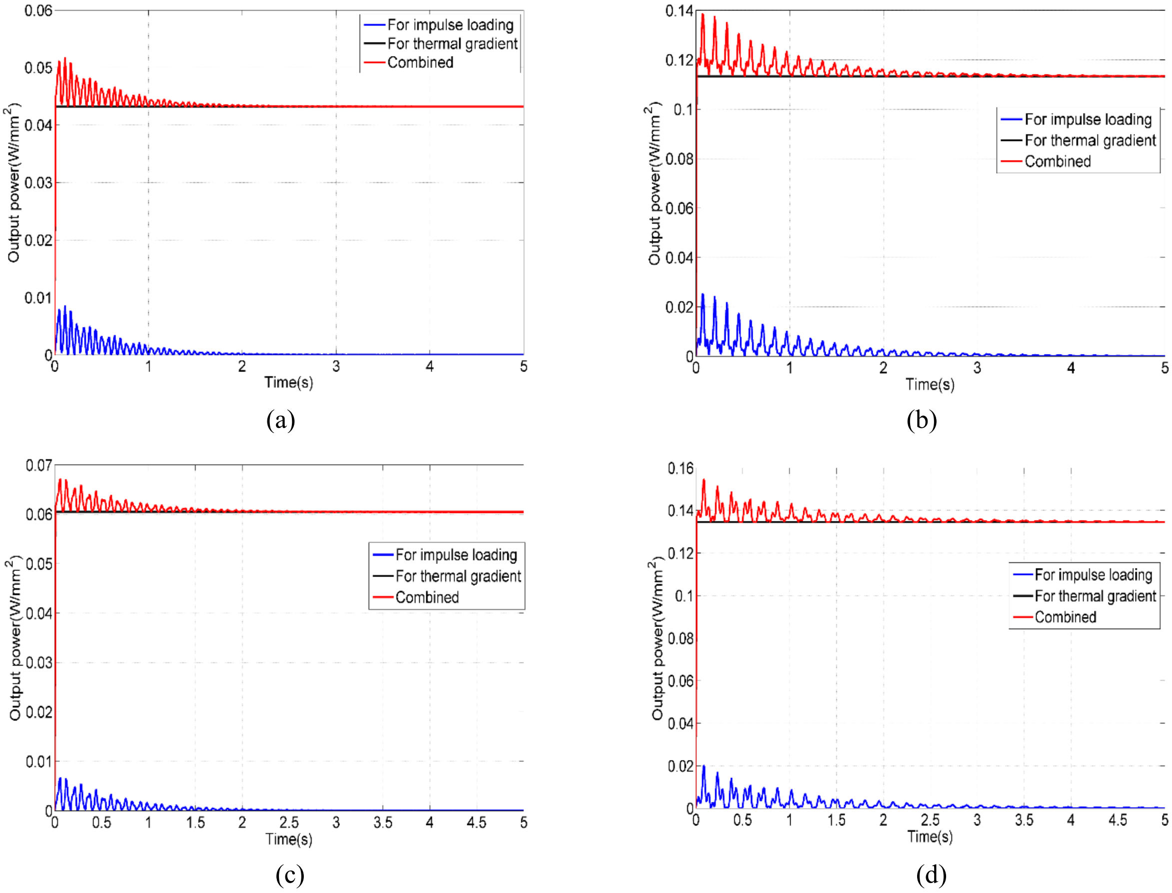

Figure 4. Output power responses of piezolaminated beam with both impulse and thermal loading for (a) cb=0.3, ch=0.3 (b) cb=0.3, ch=0.7 (c) cb=0.7, ch=0.3 (d) cb=0.7, ch=0.7

For the baseline configuration (c_b =0.3, c_h=0.3), the output power increases dramatically from 0.01 W/mm² under purely mechanical loading to 0.06 W/mm² under combined thermal-mechanical loading, representing a 500% enhancement. This substantial amplification highlights the significant contribution of thermally-induced strain to the piezoelectric energy conversion process. When the height taper coefficient increases to c_h=0.7 while maintaining c_b=0.3, the output power under combined loading reaches 0.14 W/mm², compared to 0.03 W/mm² under purely mechanical excitation. This represents a 366% increase, slightly lower than the baseline configuration's relative enhancement but yielding significantly higher absolute power. The analysis indicates that approximately 78% of the total power generation in this configuration can be attributed to the thermal gradient contribution. For the configuration with increased width taper

(c_b=0.7, c_h =0.3), the output power under combined loading reaches 0.066 W/mm², compared to 0.008 W/mm² under purely mechanical excitation. This represents an 825% increase, demonstrating the highest relative enhancement among all configurations. This remarkable amplification suggests that increased width tapering creates particularly favorable conditions for thermoelectric coupling in the piezolaminated structure.

The most striking results emerge from the configuration with both increased width and height tapers (c_b=0.7, c_h =0.7), where output power under combined loading reaches 0.15 W/mm², compared to 0.02 W/mm² under purely mechanical excitation. This represents a 650% increase, with thermal effects contributing approximately 87% of the total power generation. This configuration achieves the highest absolute power output, making it the optimal geometry for energy harvesting applications among the tested variants. These findings reveal several critical insights for piezoelectric energy harvester design. First, the thermal gradient contribution to power generation significantly outweighs the mechanical contribution across all configurations, suggesting that thermal energy harvesting represents an underexploited resource in conventional piezoelectric systems. Second, width tapering appears to create more favorable conditions for thermal-mechanical coupling than height tapering, as evidenced by the higher relative enhancement in the (c_b=0.7, c_h =0.3) configuration. The synergistic interaction between width and height tapering manifests differently in power generation compared to displacement or voltage responses. While the highest absolute power is maximized with both parameters (c_b=0.7, c_h =0.7), the relative contribution of thermal effects varies non-linearly across configurations. This suggests complex interactions between beam geometry, strain distribution, and piezoelectric coupling that merit further investigation.

From an applications perspective, these results demonstrate that FG piezolaminated tapered beams can effectively harvest energy from ambient thermal gradients in addition to mechanical vibrations. The optimal configuration (c_b=0.7, c_h =0.7) producing 0.15 W/mm² represents sufficient power density for many low-power electronic applications, particularly in self-powered sensor systems. These findings provide valuable design guidelines for maximizing energy harvesting efficiency in smart structures. Engineers should consider not only mechanical response optimization but also thermal-mechanical coupling effects when designing piezoelectric energy harvesters. Furthermore, deliberately introducing or leveraging environmental thermal gradients could substantially enhance system performance beyond what would be possible through mechanical excitation alone.

5. CONCLUSIONS

This study examined the vibrational energy harvesting potential of axially functionally graded nonprismatic piezolaminated beams for automotive applications. A multi-physics finite element model analyzed the electromechanical response of tapered cantilever beams with varying width (cb) and height (ch) taper coefficients under mechanical and thermal-mechanical loading conditions. Four configurations with taper coefficients of 0.3 and 0.7 were tested with a 50°C temperature gradient. Results showed that taper parameters significantly influenced performance, with height tapering having a greater impact on displacement (0.003-0.012 mm), while voltage generation exhibited sensitivity to both parameters. The optimized configuration (cb=0.7, ch=0.7) achieved 340 V/mm compared to 140 V/mm in the baseline configuration. Most notably, power output increased dramatically under combined loading—the baseline configuration showed a 500% increase from 0.01 to 0.06 W/mm², while the optimized configuration reached 0.15 W/mm², representing a 650% increase with thermal effects contributing approximately 87% of total power generation. These findings suggest that strategic placement near vehicle heat sources could substantially enhance energy conversion efficiency, making these systems promising for powering automotive sensors and monitoring systems. Future research could explore non-linear gradation patterns, hybrid systems, MEMS implementation, and machine learning optimization techniques.

ACKNOWLEDGEMENT

The authors gratefully acknowledge the support and encouragement received from DRIEMS University and the guidance of our mentors throughout this research. We also extend our thanks to all collaborators and reviewers whose valuable insights enriched this work. Their contributions have been instrumental in the successful completion and publication of this journal article.

CONFLICT OF INTEREST

The authors declare no conflict of interest.

AUTHOR CONTRIBUTIONS

A. R. Biswal conducted conceptualization, design methodology, developed the core computational models, conducted formal analysis, conducted validation, analyzed simulation and conducted writing original draft;

D. R. Biswal conducted supervision, conducted data curation, designed methodology, conducted conceptualization, conducted writing - review & editing, revised the manuscript, managed software, checked visualization, and conducted writing-review and editing; all authors had approved the final version.

REFERENCES

[1] A. Ali, S. Iqbal, and X. Chen, "Recent advances in piezoelectric wearable energy harvesting based on human motion: Materials, design, and applications," *Energy Strategy Reviews*, vol. 53, p. 101422, 2024.

[2] A. Aabid, M. A. Raheman, Y. E. Ibrahim, A. Anjum, M. Hrairi, B. Parveez, et al., "A systematic review of piezoelectric materials and energy harvesters for industrial applications," *Sensors*, vol. 21, no. 12, p. 4145, 2021.

[3] C. Covaci and A. Gontean, "Piezoelectric energy harvesting solutions: A review," *Sensors*, vol. 20, no. 12, p. 3512, 2020.

[4] M. Askari, E. Brusa, and C. Delprete, "Vibration energy harvesting via piezoelectric bimorph plates: an analytical model," *Mechanics of Advanced Materials and Structures*, vol. 30, no. 23, pp. 4764–4785, 2023.

[5] M. Iqbal, M. M. Nauman, F. U. Khan, P. E. Abas, Q. Cheok, A. Iqbal, et al., "Vibration-based piezoelectric, electromagnetic, and hybrid energy harvesters for microsystems applications: A contributed review," *International Journal of Energy Research*, vol. 45, no. 1, pp. 65–102, 2021.

[6] V. N. Burlayenko, R. Kouhia, and S. D. Dimitrova, "One-dimensional vs. three-dimensional models in free vibration analysis of axially functionally graded beams with nonuniform cross-sections," *Mechanics of Composite Materials*, vol 60, pp. 83–102, 2024.

[7] N. Wu, B. Bao, and Q. Wang, "Review on engineering structural designs for efficient piezoelectric energy harvesting to obtain high power output," *Engineering Structures*, vol. 235, p. 112068, 2021.

[8] T. Li and P. S. Lee, "Piezoelectric energy harvesting technology: From materials, structures, to applications," *Small Structures*, vol. 3, no. 3, p. 2100128, 2022.

[9] J. Wang, C. Han, S.H. Jo, W. Xu, and H. Tian, "Enhanced flow induced vibration piezoelectric energy harvesting performance by optimizing tapered beam," *Ocean Engineering*, vol. 300, p. 117459, 2024.

[10] M. N. Hasan, M. A. Muktadir, and M. Alam, "Comparative study of tapered shape bimorph piezoelectric energy harvester via finite element analysis," *Forces in Mechanics*, vol. 9, p. 100131, 2022.

[11] D. Cao, Y. Gao, M. Yao, and W. Zhang, "Free vibration of axially functionally graded beams using the asymptotic development method," *Engineering Structures*, vol. 173, pp. 442–448, 2018.

[12] R. Singh and P. Sharma, "Free vibration analysis of axially functionally graded tapered beam using harmonic differential quadrature method," *Materials Today: Proceedings*, vol. 44, pp. 2223–2227, 2021.

[13] A. R. Biswal, T. Roy, and R. K. Behera, "Optimal vibration energy harvesting from nonprismatic piezolaminated beam," *Smart structures and systems*, vol. 19, no. 4, pp. 403–413, 2017.

[14] X. Yang, T. Zhang, Y. Shen, Y. Liu, V. C. Bui, and D. Qiu, "Trade-off analysis of the energy-harvesting vehicle suspension system employing inerter element," *Energy*, vol. 308, p. 132841, 2024.

[15] S. Touairi and M. Mabrouki, "Vibration harvesting integrated into vehicle suspension and bodywork," *Indonesian Journal of Electrical Engineering and Computer Science*, vol. 23, no. 1, pp. 188–196, 2021.

[16] S. Kumar, H. Roy, A. Mitra, and K. Ganguly, "Dynamic analysis of bi-directional functionally graded beam with geometric nonlinearity," *Journal of Vibration Engineering & Technologies*, vol. 12, no. 3, pp. 3051–3067, 2024.

[17] K. Xie, Y. Wang, and T. Fu, "Dynamic response of axially functionally graded beam with longitudinal–transverse coupling effect," *Aerospace Science and Technology*, vol. 85, pp. 85–95, 2019.

[18] M. Alimoradzadeh, M. Salehi, and S. M. Esfarjani, "Nonlinear dynamic response of an axially functionally graded (AFG) beam resting on nonlinear elastic foundation subjected to moving load," *Nonlinear Engineering*, vol. 8, no. 1, pp. 250–260, 2019.

[19] D. K. Nguyen, A. N. T. Vu, N. A. T. Le, and V. N. Pham, "Dynamic behavior of a bidirectional functionally graded sandwich beam under nonuniform motion of a moving load," *Shock and Vibration*, vol. 2020, pp. 1–15, 2020.

[20] I. Esen, "Dynamic response of a functionally graded Timoshenko beam on two-parameter elastic foundations due to a variable velocity moving mass," *International Journal of Mechanical Sciences*, vol. 153, pp. 21–35, 2019.

[21] S. Kundu and H. B. Nemade, "Piezoelectric vibration energy harvester with tapered substrate thickness for uniform stress," *Microsystem Technologies*, vol. 27, pp. 105–113, 2021.

[22] A. Tati, "Finite element analysis of thermal and mechanical buckling behavior of functionally graded plates," *Archive of Applied Mechanics*, vol. 91, no. 11, pp. 4571–4587, 2021.

[23] R. Eshtehardiha, R. Tikani, and S. Z. Rad, "Experimental and numerical investigation of energy harvesting from double cantilever beams with internal resonance," *Journal of Sound and Vibration*, vol. 500, p. 116022, 2021.

[24] J. R. Cheng and M. Gen, "Parallel genetic algorithms with GPU computing," in Industry 4.0-Impact on Intelligent Logistics and Manufacturing, IntechOpen, 2020.

[25] Y.C. Chuang, C.T. Chen, and C. Hwang, "A simple and efficient real-coded genetic algorithm for constrained optimization," *Applied Soft Computing*, vol. 38, pp. 87–105, 2016.

[26] Y. Li, K. Tao, B. George, and Z. Tan, "Harvesting vibration energy: Technologies and challenges," *IEEE Industrial Electronics Magazine*, vol. 15, no. 1, pp. 30–39, 2020.

[27] A. R. Biswal, T. Roy, and R. K. Behera, "Geometric nonlinear finite element and genetic algorithm based optimal vibration energy harvesting from nonprismatic axially functionally graded piezolaminated beam," *Journal of Vibration and Control*, vol. 24, no. 10, pp. 1889–1909, 2018.

[28] J. S. Yang and R. C. Batra, "Free vibrations of a linear thermopiezoelectric body," *Journal of Thermal Stresses*, vol. 18, no. 2, pp. 247–262, 1995.

[29] J. N. Reddy, An Introduction to Nonlinear Finite Element Analysis: with applications to heat transfer, fluid mechanics, and solid mechanics. Oxford University Press, 2015.

[30] W.S. Hwang and H. C. Park, "Finite element modeling of piezoelectric sensors and actuators," *American Institute of Aeronautics and Astronautics Journal*, vol. 31, no. 5, pp. 930–937, 1993.

[31] H. S. Tzou and R. Ye, "Analysis of piezoelastic structures with laminated piezoelectric triangle shell elements," *American Institute of Aeronautics and Astronautics Journal*, vol. 34, no. 1, pp. 110–115, 1996.